

Ionospheric storm effects in the nighttime E region caused by neutralized ring current particles

R. Bauske¹, S. Noël², and G. W. Prölss

Institut für Astrophysik und Extraterrestrische Forschung, Universität Bonn, Auf dem Hügel 71, D-53121 Bonn, Germany

¹Now at: Space Physics Research Laboratory, Department of Atmospheric, Oceanic and Space Science, University of Michigan, 2455 Hayward Street, Ann Arbor, Michigan, 48109–2143, USA

²Now at: Institut für Fernerkundung, Physik und Elektrotechnik, Fachbereich 1, Universität Bremen, Postfach 33 04 40, D-28334 Bremen, Germany

Received: 13 May 1996 / Revised: 18 November 1996 / Accepted: 19 November 1996

Abstract. During magnetic storms an anomalous increase in the ionization density of the nighttime E region is observed at low and middle latitudes. It has been suggested that this effect is caused by the precipitation of neutralized ring current particles. Here a coupled ring current decay–ionosphere model is used to confirm the validity of this explanation.

1 Introduction

The electron density in the lower ionosphere is known to increase during magnetically disturbed nights (e.g. Haubert, 1959; Wakai, 1967; Rowe, 1973, 1974; Shen *et al.*, 1976; Voss and Smith, 1979; Batista *et al.*, 1991; Morton and Mathews, 1993). Figure 1 illustrates this effect using incoherent scatter data from Arecibo (Rowe, 1974). Compared are electron density profiles obtained near midnight during quiet and severely disturbed conditions. As is evident, there is a very significant storm induced increase of the ionization density in the 110 to 250 km altitude range.

Hirao *et al.* (1965) suggested energetic particle precipitation as a possible cause of these density enhancements, however without specifying the particle species, their energy or origin. Later Lyons and Richmond (1978) and Tinsley (1979) argued that these particles are most likely neutral atoms in the energy range 1–100 keV which originate from the ring current. The disturbance scenario envisaged by these authors is illustrated in Fig. 2. During magnetic storms a considerable amount of energy is injected into the ring current of the inner magnetosphere. Part of this energy is transmitted to the upper atmosphere by neutralized ring current particles. It is the precipitation of these neutralized ring current particles which is held responsible for the ionization density enhancements at middle and lower latitudes. The

associated production rate was estimated by Lyons and Richmond (1978) to be of the order of $10\text{--}100\text{ cm}^{-3}\text{ s}^{-1}$ at 30° magnetic latitude during the main phase of a larger storm. This estimate was based on particle flux measurements by Mizera and Blake (1973) and model calculations by Prölss *et al.* (1973) and Prölss (1973). Production rates of this magnitude were previously shown to be sufficient to explain the E-region density enhancements observed at Wallops Island (Smith *et al.*, 1974).

The present study combines a ring current decay model and an ionospheric model to investigate the disturbance scenario mentioned above more closely. First, a Monte Carlo type simulation is used to calculate the ionization produced by precipitated neutralized ring current particles. Subsequently, this production rate is fed into an ionospheric model to determine the resulting density enhancements at E region heights.

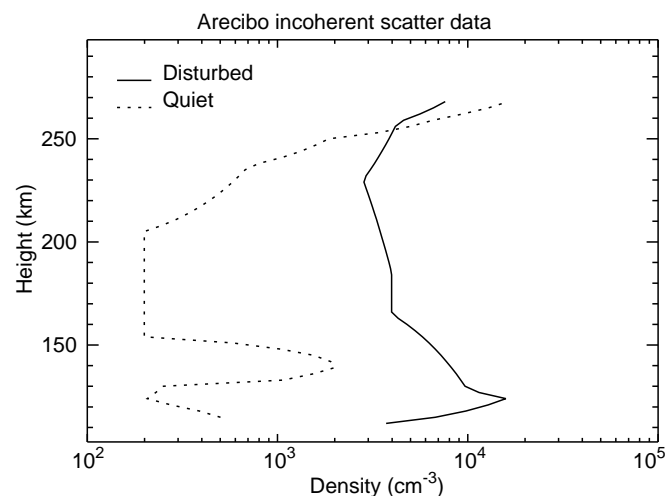


Fig. 1. Electron density profiles observed at Arecibo during the magnetically quiet night of November 29, 1972 ($K_p \approx 2$) and during the magnetically disturbed night of October 31, 1972 ($K_p \approx 8$). The time of observation was 23:30 LT (Rowe, 1974)

2 Ionization production by neutralized ring current particles

To determine the ionization production by neutralized ring current particles, the decay of the magnetospheric ring current is simulated using a Monte Carlo type calculation. The details of this simulation were already discussed by Noël and Prölss (1993). To summarize briefly, at the beginning of a simulation a large number of ring current ions is located in the inner magnetosphere. Here, these particles gyrate around and oscillate along the magnetic field lines until they are neutralized in a charge exchange collision. Once neutralized, they are no longer constrained to follow the magnetic field lines but continue their travel along a straight trajectory away from the ring current. If they head towards Earth, they impinge upon the denser atmosphere and interact with gas particles via elastic and inelastic collisions. In each of these collisions, they lose some of their energy, part of which is consumed in ionizing collisions. This way the ring current particles random walk through the upper atmosphere until they have dissipated their energy or until they have escaped from the denser atmosphere. Complications arise from the fact that the incident particles themselves may be reionized, upon which they resume their spiral motion along the local magnetic field line until they are neutralized again, see Fig. 3. Furthermore, the energy transfer in a collision may be so large that a secondary energetic particle is generated which in turn may produce a tertiary energetic particle, and so on, see Fig. 4. These higher order energetic particles play an important role in the energy dissipation process and are treated in the same manner as the primary particles.

The most recent version of our simulation algorithm contains a number of improvements over our earlier

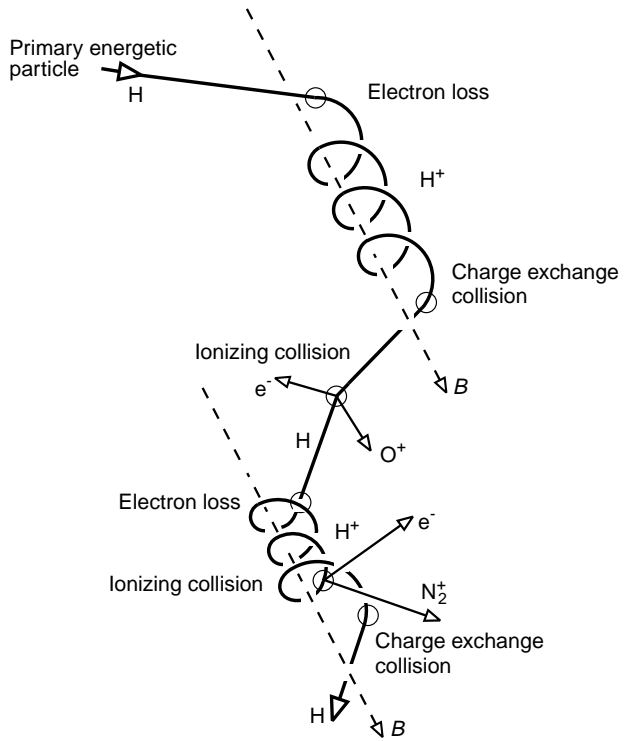


Fig. 3. Energetic hydrogen particle trajectory in the upper atmosphere. The vector B indicates the direction of the local magnetic field

model (Noël and Prölss, 1993). For example, the initial radial distribution of the ring current ions is now taken directly from satellite measurements. Also the pitch angle distribution is now assumed to be isotropic at all points along the magnetic field line, in agreement with the observations. Furthermore, the initial position of the ring current particles is fixed by choosing, within the bounce periods, the time at which the particles first cross

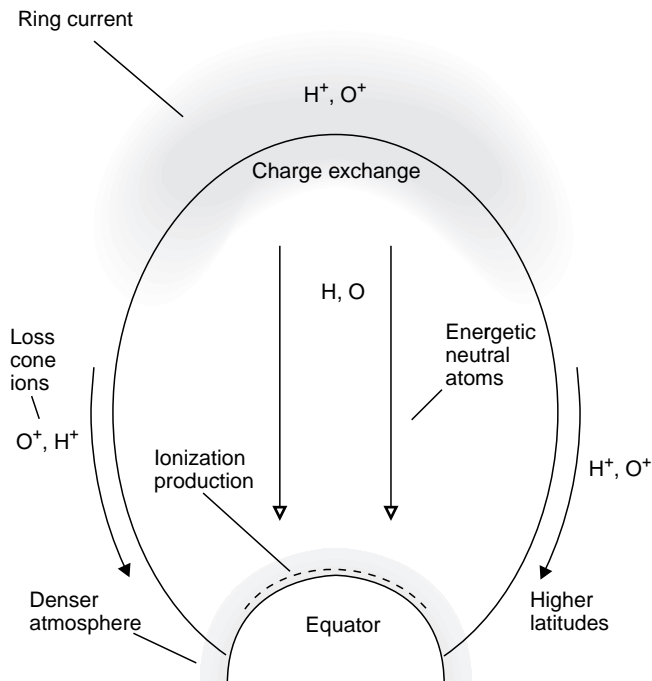


Fig. 2. Ionization production by neutralized ring current particles

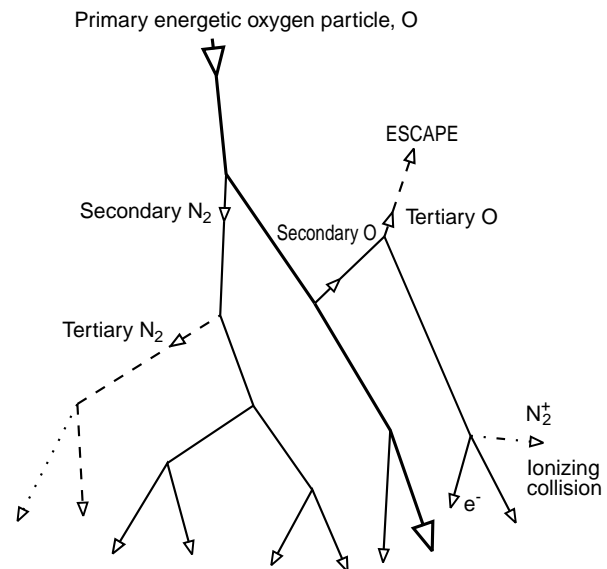


Fig. 4. Energetic oxygen particle trajectory in the upper atmosphere

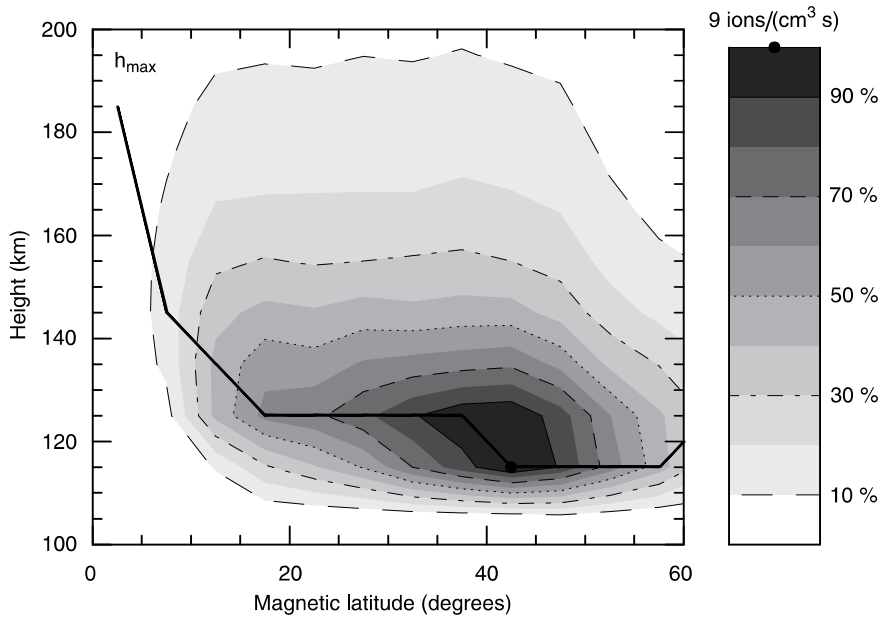


Fig. 5. Ionization production by neutralized ring current particles. The production rates are averages which refer to the first 4 hours of the simulation, excluding the initial 5 min which are dominated by the decay of loss cone particles. The maximum production rate is $9 \text{ ions/cm}^3 \text{ s}$. The location of this maximum is indicated by a solid dot. The solid line h_{max} indicates the height of the maximum ionization production as a function of magnetic latitude

the equatorial plane at random. This determines the location of the particles along the magnetic field line at time $t = 0$. We have also updated our charge exchange cross sections. Instead of extrapolating the measurements of Fite (1964) to higher energies, we now use the cross sections given in Fok *et al.* (1993). Finally, we now also allow for the ionization of H, O, and N_2 particles by energetic H and O ions. The changes above lead to a general reduction of the rate of energy deposition in the upper atmosphere and also shift the location of maximum energy injection towards higher latitudes.

To run the Monte Carlo model, the properties of the ring current have to be specified. Our first simulation is based on AMPTE satellite measurements recorded during the magnetic storm on April 20/21, 1985 at about 22:00 local time (see Gloeckler and Hamilton, 1987). These measurements refer to Dst indices in the range -89 to -127 nT. The result of this simulation is shown in Figure 5. The average ionization production rates presented in this figure apply to the first 4 hours of the simulation excluding the initial five minutes which are dominated by the decay of loss cone ions. As is evident, significant production rates are attained in an extended region between 25 and 50 degrees magnetic latitude and 115 to 135 km altitude. Here the production rate exceeds $6 \text{ ions/cm}^3 \text{ s}$. The exact distribution depends somewhat on the time interval considered. Thus during the first 55 minutes, the time averaged maximum production rate is approximately $15 \text{ ions/cm}^3 \text{ s}$, whereas during the last two hours it decreases to about $7 \text{ ions/cm}^3 \text{ s}$. At the same time, the center of ionization production moves from 57.5° to 42.5° magnetic latitude.

The relatively low altitude of the maximum indicates that it is mostly the hydrogen particle component which is responsible for the ionization production. This is understandable since the hydrogen particles carry most of the ring current energy at the time of the AMPTE measurements (22:00–01:00 UT) and their ionizing

cross sections are larger than those of the oxygen particles.

3 E region effects

To evaluate the significance of the ionization production by precipitated neutralized ring current particles, the results of the Monte Carlo simulation are fed into an ionospheric model. The general properties of this model are summarized in Table 1. The ionospheric simulation is performed for a location near Arecibo at 30° magnetic latitude and for conditions on April 20, 1985, the day of the ring current measurements. Since these measurements refer to 22:00 LT, this time was chosen to switch on the ring current ionization source. One and a half hours later (i. e. at the time of the Arecibo measurements at 23:30 LT) the ionization density in the E and F1 regions has increased significantly, as is illustrated in Fig. 6. For comparison, this figure also shows the results of a model run for the same general conditions but without the additional ring current ionization source. Obviously, there is good qualitative agreement with the observations. By adjusting the wind profile and the nighttime radiation source, this agreement could be further improved. This, however, is not of interest here. What is important is that our simulation reproduces the storm-induced enhancement of the ionization density in E and F1 regions, which at 180 km altitude reaches a factor of more than five. The temporal development of this density increase is illustrated in Figure 7.

In both the quiet time and the storm simulations, downward-moving tidal ionization layers occur in the height range 180 to 115 km. Of course, these layers have nothing to do with the ring current ionization source. They are produced by shears in the meridional neutral winds, as specified by the wind model of Hedin *et al.* (1996). The additional ionization produced by ring

Table 1. Ionospheric Model

- Solves the continuity equation

$$\frac{\partial n}{\partial t} = Q - L(n) - \frac{\partial(nu_z)}{\partial z}$$

for the ion species

O^+ , O_2^+ , N_2^+ , NO^+ , N^+ , $O^+(^2D)$, and $O^+(^2P)$

in the height range 90 to 600 km

- Production rate Q :

Daytime EUV source: Model EUVAC of Richards *et al.* (1994)

Nighttime EUV source: Updated model of Ogawa and Tohmatsu (1966)

Absorption and ionization cross sections: Richards *et al.* (1994)

Ring current ionization source: Monte Carlo simulation

- Loss rate $L(n)$:

Chemical reaction rate coefficients:

Torr and Torr (1982) without N_2^{+*} (vib),

Gérard (1992), and references therein

- Transport $\partial(nu_z)/\partial z$

Ambipolar diffusion

Wind-induced drifts: HWM 93 (Hedin *et al.*, 1996)

Topside flux: $2 \times 10^8 \text{ cm}^{-2}\text{s}^{-1}$ downward

- Neutral atmosphere:

MSISE 90 model (Hedin, 1991)

Self-consistently calculated NO, N, and $N(^2D)$ densities

- Electron temperature: Solution of the electron energy equation

$$\frac{\partial T_e}{\partial t} + \bar{u}_{e\parallel} \text{grad } T_e + 2/3 T_e \text{div } \bar{u}_{e\parallel}$$

$$= \frac{2}{3k n_e} (Q_e - L_e - \text{div} \bar{q}_{e\parallel})$$

- Ion temperature: Model of Titheridge (1993):

$$T_i = T_n + \frac{T_e - T_n}{1 + \left(\frac{0.72T_n}{h}\right)^6}$$

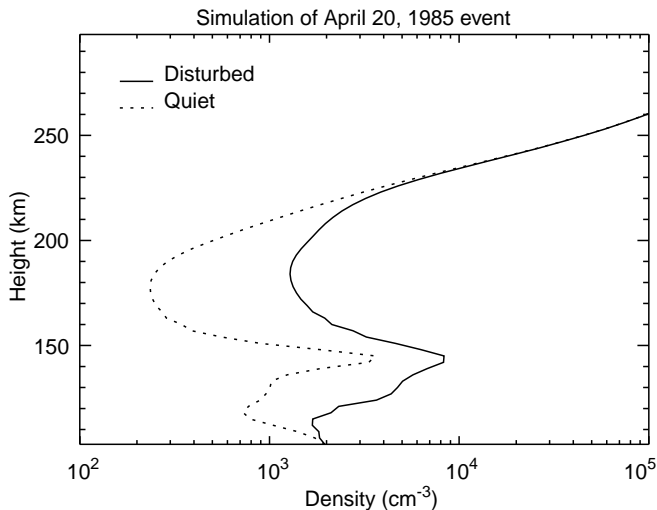


Fig. 6. Electron density profiles calculated for a location near Arecibo at 30° magnetic latitude with (disturbed) and without (quiet) the ring current ionization source. The model ring current decay was assumed to begin at 22:00 LT, and the electron density profiles were obtained 1 1/2 hours later at 23:30 LT. The general conditions apply to the day of the ring current measurements, i.e. April 20, 1985

current particles enhances these layers and also reduces their downward motion. In fact, a slight stabilization at heights near 130 km may be noticed in Fig. 7.

Compared with the observations shown in Fig. 1, the simulated storm time ionization density appears to be somewhat too small. It should be noted, however, that during the Arecibo measurements the Dst index reached values of nearly -200 nT, whereas our simulation results are based on ring current data recorded at Dst values between -89 and -127 nT. To check on the magnetic activity dependence of our results, an additional simulation is performed. This time, AMPTE satellite measurements obtained during the storm of February 9, 1986 are used as input to the Monte Carlo simulation. These measurements refer to Dst indices in the range between -202 and -286 nT. The model ring current is injected at 21:00 LT, i.e. at the time of the AMPTE measurements. Again, the ionization production rates predicted by the Monte Carlo simulation are fed into the ionospheric model. In Fig. 8 the resulting ionization densities at 21:30 LT are compared to the results of a reference simulation performed without the ring current ionization source. As is evident, the ionization density now even exceeds that observed at Arecibo during the October storm. Again, it is primarily the quiet-time behaviour which is not reproduced very well.

4 Summary

This study investigates the effect neutralized ring current particles have on the ionization density of the nighttime E region. First, a Monte Carlo type simulation is used to determine the additional ionization produced by these particles. It is found that the production rate maximizes in an extended region between 25 and 50 degrees magnetic latitude and in an altitude range between 115 to 135 km. For moderate magnetic activity ($-89 \text{ nT} \geq \text{Dst} \geq -127 \text{ nT}$), peak production rates exceed $15 \text{ ions/cm}^3\text{s}$. Fed into an ionosphere model, these production rates cause the nighttime E-region density to increase by a factor of up to 5. For more severely disturbed conditions ($-202 \text{ nT} \geq \text{Dst} \geq -286 \text{ nT}$), the E region density becomes larger than $5 \times 10^3 \text{ cm}^{-3}$, in good agreement with the observations. It is concluded that indeed the precipitation of neutralized ring current particles is responsible for the positive ionospheric storm effects observed in the nighttime E region at middle and lower latitudes, as was suggested by Lyons and Richmond (1978) and Tinsley (1979).

Acknowledgements. We thank George Gloeckler and the World Data Center-A for Rockets and Satellites for providing the AMPTE/CCE data. This research was supported by the Deutsche Forschungsgemeinschaft under grants Pr 276/6-2, Pr 276/3-1,2 and No 285/1-1.

Topical Editor D. Alcaydé thanks R. L. Lyons and M. -C. Fok for their help in evaluating this paper.

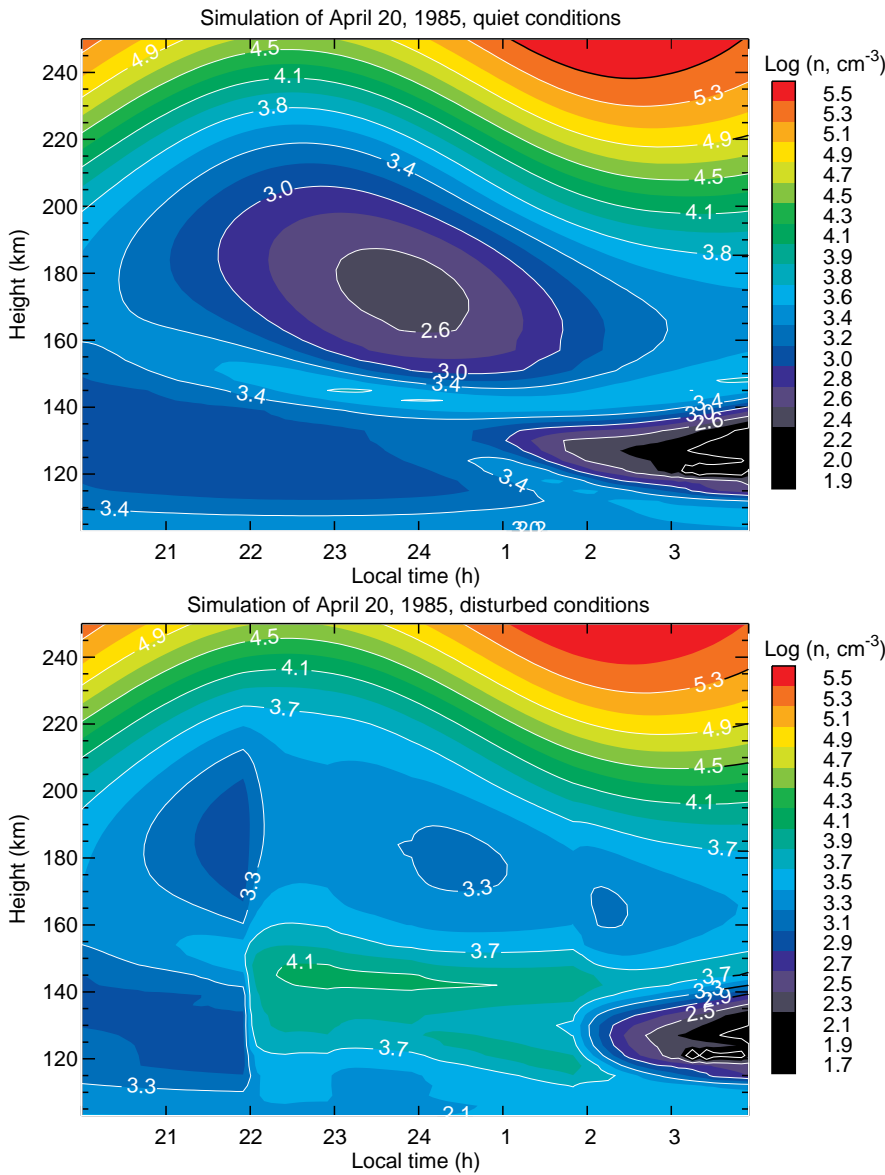


Fig. 7. Contour plots of the electron densities obtained in the simulations for April 20, 1985. A tidal layer moves from an altitude of 180 km downward to an altitude of 115 km. The density of this layer is enhanced due to the additional ionization production by precipitated ring current particles. Also the valley between this layer and the lower F-region is filled in by this additional ionization

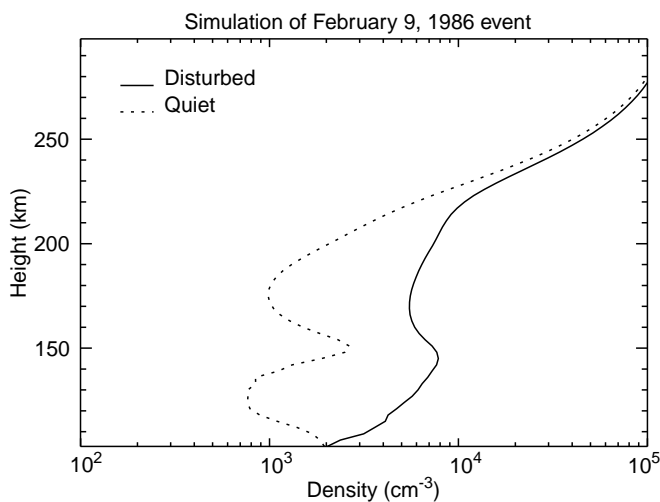


Fig. 8. Electron density profiles calculated for February 9, 1986 for a location close to Arecibo, again with (disturbed) and without (quiet) the ring current ionization source. Here, the model ring current was injected at 21:00 LT, and the electron density profiles were obtained 1/2 hour later at 21:30 LT

References

Batista, I. S., E. R. de Paula, M. A. Abdu, N. B. Trivedi, and M. E. Greenspan, Ionospheric effects of the March 13, 1989, magnetic storm at low and equatorial latitudes, *J. Geophys. Res.*, **96**, 13943–13952, 1991.

Fite, W. L., Charge exchange transfer and ion-atom interchange collisions above thermal energies, *Ann. Geophys.*, **20**, 47–73, 1964.

Fok, M.-C., J. U. Kozyra, A. F. Nagy, C. E. Rasmussen, and G. C. Khazanov, Decay of equatorial ring current ions and associated aeronomical consequences, *J. Geophys. Res.*, **98**, 19381–19393, 1993.

Gérard, J. C., Thermospheric odd nitrogen, *Planet. Space Sci.*, **40**, 337–353, 1992.

- Gloeckler, G., and D. C. Hamilton**, AMPTE ion composition results, *Phys. Scr.*, **T18**, 73–84, 1987.
- Haubert, A.**, L'ionisation nocturne de la région-E et l'activité géomagnétique, *J. Atmos. Terr. Phys.*, **15**, 84–87, 1959.
- Hedin, A. E.**, Extension of the MSIS thermosphere model into the lower and middle atmosphere, *J. Geophys. Res.*, **96**, 1159–1172, 1991.
- Hedin, A. E., E. L. Fleming, A. H. Manson, F. J. Schmidlin, S. K. Avery, R. R. Clark, S. J. Franke, G. J. Fraser, T. Tsuda, F. Vial, and R. A. Vincent**, Empirical model for the upper, middle and lower atmosphere, *J. Atmos. Terr. Phys.*, **58**, 1421–1447, 1996.
- Hirao, K., N. Wakai, K. Sawada, T. Hikosaka, K. Yano, and K. Maeda**, Some evidences of the particle effects on the ionosphere at middle latitudes, *Space. Res.*, **5**, 1058–1070, 1965.
- Lyons, L. R., and A. D. Richmond**, Low-latitude E region ionization by energetic ring current particles, *J. Geophys. Res.*, **83**, 2201–2204, 1978.
- Mizera, P. F., and J. B. Blake**, Observations of ring current protons at low latitudes, *J. Geophys. Res.*, **78**, 1058–1062, 1973.
- Morton, Y. T., and J. D. Mathews**, Effects of the 13–14 March 1989 geomagnetic storm on the E-region tidal ion layer structure at Arecibo during AIDA, *J. Atmos. Terr. Phys.*, **55**, 467–485, 1993.
- Noël, S., and G. W. Prölss**, Heating and radiation production by neutralized ring current particles, *J. Geophys. Res.*, **98**, 17317–17325, 1993.
- Ogawa, T., and T. Tohmatsu**, Photoelectronic processes in the upper atmosphere, II. The hydrogen and helium ultraviolet glow as an origin of the nighttime ionosphere, *Rep. Ionosph. Space. Res. Japan*, **20**, 395–417, 1966.
- Prölss, G. W.**, Radiation production and energy deposition by ring current protons dissipated by the charge-exchange mechanism, *Ann. Geophys.*, **29**, 503–508, 1973.
- Prölss, G. W., K. Najita, and P. C. Yuen**, Heating of the low-latitude upper atmosphere caused by the decaying magnetic storm ring current, *J. Atmos. Terr. Phys.*, **35**, 1889–1901, 1973.
- Richards, P. G., J. A. Fennelly, and D. G. Torr**, EUVAC: A solar EUV flux model for aeronomic calculations, *J. Geophys. Res.*, **99**, 8981–8992, 1994.
- Rowe, J. F., Jr.**, A statistical summary of Arecibo nighttime E region observations, *J. Geophys. Res.*, **78**, 6811–6817, 1973.
- Rowe, J. F., Jr.**, Magnetic activity variations of the nighttime E region at Arecibo, *Radio Sci.*, **9**, 175–182, 1974.
- Shen, J. S., W. E. Swartz, D. T. Farley, and R. M. Harper**, Ionization layers in the nighttime E region valley above Arecibo, *J. Geophys. Res.*, **81**, 5517–5526, 1976.
- Smith, L. G., M. A. Geller, and H. D. Voss**, Energetic electrons in the mid-latitude nighttime E-region, *J. Atmos. Terr. Phys.*, **36**, 1601–1612, 1974.
- Tinsley, B. A.**, Energetic neutral atom precipitation during magnetic storms: Optical emission, ionization, and energy deposition at low and middle latitudes, *J. Geophys. Res.*, **84**, 1855–1864, 1979.
- Titheridge, J. E.**, Atmospheric winds calculated from diurnal changes in the mid-latitude ionosphere, *J. Atmos. Terr. Phys.*, **55**, 1637–1659, 1993.
- Torr, M. R., and D. G. Torr**, The role of metastable species in the thermosphere, *Geophys. Res. Lett.*, **6**, 771–774, 1982.
- Voss, H. D., and L. G. Smith**, Nighttime ionization by energetic particles at Wallops Island in the altitude region 120 to 200 km, *Geophys. Res. Lett.*, **6**, 93–96, 1979.
- Wakai, N.**, Quiet and disturbed structure and variations of the nighttime E-region, *J. Geophys. Res.*, **72**, 4507–4517, 1967.